

Reinforcement of Elastomeric Networks by Fillers

Liliane BOKOBZA

Laboratoire de Physico-Chimie Structurale et Macromoléculaire, ESPCI, 10 rue Vauquelin, 75231 Paris, Cedex 05, France

SUMMARY: Although numerous investigations have been devoted to the analysis of filled systems, the mechanisms of the reinforcement have not been completely clarified. The present paper attempts to recall, through new experimental data, some of the basic mechanisms of filler reinforcement. The basic processes giving rise to the increase in the elastic modulus, generally observed by a filler addition in an elastomeric medium, are discussed in the light of mechanical measurements and of recent results based on measurements of chain orientation.

Introduction

The commercial applications of elastomers require the use of solid fillers to obtain an improvement of their mechanical properties. Although filled systems have been used for many years, the mechanisms of reinforcement are not completely understood.

Even the definition of the term "reinforcement" is difficult because it depends somewhat on the experimental conditions and on the intended effects of the filler addition. A practical definition of reinforcement is the improvement in the service life of a rubber article.

Generally, reinforced elastomers show an increase in modulus, hardness, tensile strength, abrasion and tear resistance as well as resistance to fatigue and cracking. Frequently, however, only some of these properties are significantly improved by reinforcing fillers.

A filled network may be regarded as a two-phase-system of rigid particles surrounded by an elastomeric network formed by flexible chains permanently linked together by chemical junctions (Fig.1).

Filler morphology such as particle size, structure and essentially surface characteristics are significant factors for reinforcing ability. The particle surface will determine the interaction between the filler and the polymer chains which is the key parameter in rubber reinforcement. In fact, a better characterization of this interfacial interaction is essential in understanding the mechanism of rubber reinforcement.

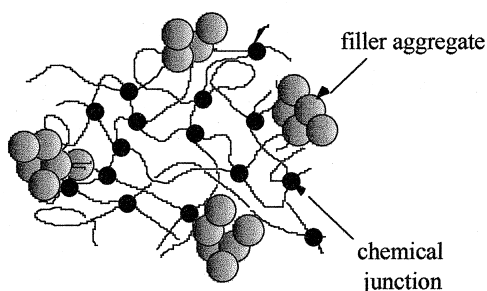


Fig. 1: Filled elastomeric network.

This interaction which leads to an adsorption of the network chains onto the particle surfaces can result from :

- physical interaction arising from long-range Van der Waals forces between the surface and the polymer,

- or chemical interaction which can be direct by chemisorption of elastomers or indirect by means of coupling agents used in the case of poor adhesive qualities of a filler for a polymer.

Coupling agents are generally bifunctional molecules which are able to establish molecular bridges at the interface between the polymer matrix and the filler surface. Several silane coupling agents are commonly used in sulfur cured compounds filled with non-black fillers. The bis(3-triethoxysilylpropyl)tetrasulfide commonly abbreviated "Si69" has widened the use of silica in rubber applications. With this kind of difunctional material, there always exists the possibility for additional network cross-linking, rather than interfacial coupling.

A poor polymer-filler interaction would result in a dewetting (or cavitation) and vacuole formation upon a significant deformation thus initiating cracks. Therefore, a strong bond between particle and matrix significantly improves reinforcement.

A number of molecular processes, most of which lack good experimental proof, have been proposed to explain filler reinforcement. Let us examine some of these processes in the light of our experimental data.

Basic mechanisms of filler reinforcement

Filler effects on elastomeric materials are not the results of a single phenomenon but several molecular mechanisms can contribute to reinforcement. In order to discuss some of the basic processes, it is interesting to start from the strain dependence of the true stress for unfilled and filled elastomeric networks, supposed to be at a same initial cross-linking level (Fig.2). One of the most characteristic feature in filler reinforcement is obviously the increase in the elastic modulus with the filler fraction.

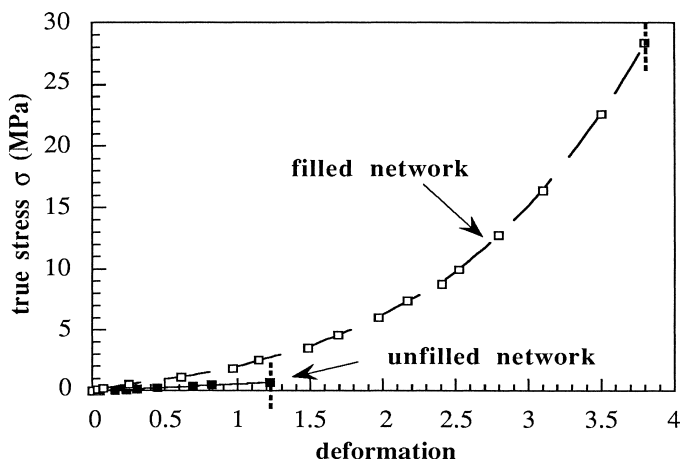


Fig.2: Typical stress-strain curves.

Mechanical effect

The first contribution to the modulus arises from the inclusion of rigid particles in the elastomeric medium. This effect is usually expressed by the Guth and Gold equation^{1,2)}:

$$G = G_0 (1 + a\phi + b\phi^2) \quad (1)$$

where G_0 is the modulus of the unfilled sample, ϕ the volume fraction of filler and a and b are numbers which depend on the geometry of the filler particles.

Filler-rubber interactions

However it is empirically known that the actual network modulus is in most cases higher than that predicted by a pure mechanical model. This result is mainly attributed to filler-rubber interactions leading to an introduction of additional cross-links into the network by the filler, thus increasing the effective degree of cross-linking.

The density of polymer-filler attachments can be evaluated independently from equilibrium swelling measurements and also by the analysis of chain orientation carried out by infrared dichroism or by birefringence.

Equilibrium swelling measurements

The well-known Flory-Rehner equation³⁾, based on the affine network model, has been widely used to estimate the network chain density reflected by the apparent molecular weight between cross-links M_c :

$$M_c = - \frac{\rho V_1 (v_2^{1/3} - 1/2v_2)}{\ln(1 - v_2) + \chi v_2^2 + v_2} \quad (2)$$

In the Flory-Rehner equation, ρ denotes the network density during formation, V_1 is the molar volume of solvent, v_2 is the volume fraction of polymer at conditions of equilibrium and χ is the interaction parameter for the solvent-polymer system.

The Flory-Rehner equation is based on an affine network model. In an affine network, the junctions points are assumed to be embedded in the network and transform affinely with macroscopic deformation, while in the phantom network model, the junction points fluctuate over time without being hindered by the presence of the neighboring chains.

As the mechanical behavior of a swollen network is closer to that of a phantom network model, the use of the Flory-Erman equation given by the following expression^{4,5)}:

$$M_c = - \frac{\rho (1 - 2/\phi) V_1 v_2^{1/3}}{\ln(1 - v_2) + \chi v_2^2 + v_2} \quad (3)$$

is more appropriate since it treats the system as a phantom network. ϕ is the junction functionality which is the number of chains which meet at one junction

Under the assumption that the filler does not swell, we can calculate the equilibrium swelling ratio of the rubber alone, which is equal to the following quantity :

$$Q_{\text{rubber}} = \frac{Q - \phi}{1 - \phi} \quad (4)$$

where ϕ is the volume fraction of filler.

The apparent increase in the cross-linking density, attributed to filler-polymer links, is reflected by the restricted swelling of the rubber by solvent with an increase in the filler fraction. The results represented in Fig.3 are related to silica-filled styrene-butadiene copolymers.

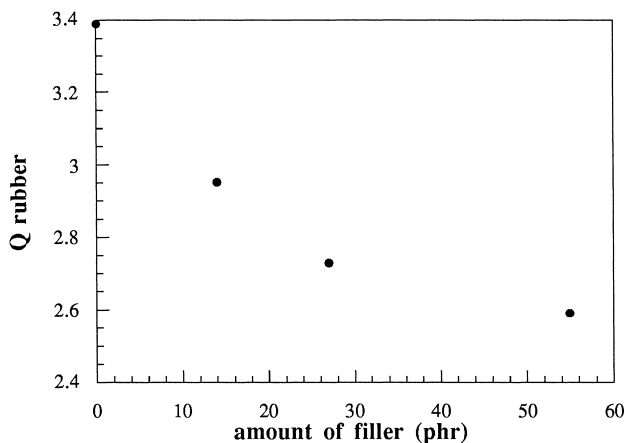


Fig.3: Dependence of rubber phase swelling on the amount of filler for styrene-butadiene copolymers filled with silanized- silica.

Measurements of chain orientation

The analysis of the orientational behavior of filled networks can provide a direct estimation of the total network chain density.

If a network is submitted to an uniaxial deformation, the polymer chains tend to orient along the direction of stretch (Fig.4).

The orientation of segments under strain may be conveniently described by the second Legendre polynomial⁶⁾ :

$$\langle P_2(\cos \theta) \rangle = \frac{1}{2} (3 \langle \cos^2 \theta \rangle - 1) \quad (5)$$

where θ is the angle between the macroscopic reference axis (usually taken as the direction of strain) and the local chain axis of the polymer (Fig.5). The angular brackets indicate an average over all molecular chains and over all possible configurations of these chains.

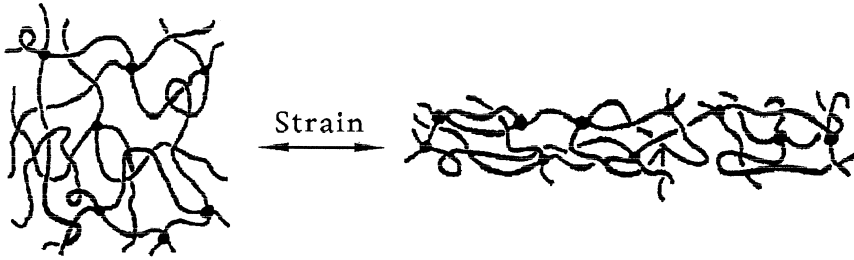


Fig.4: Orientation of network chains under strain.

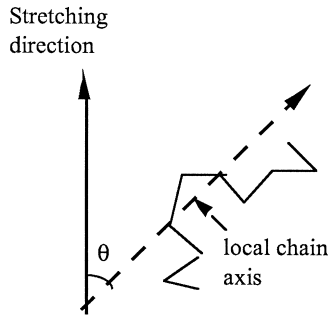


Fig.5: Definition of chain orientation.

The orientation function P_2 , which characterizes the segmental orientation in phantom and affine network models under uniaxial extension depends on the term D_0 which is called the configurational factor :

$$\langle P_2(\cos \theta) \rangle = \mathcal{P} D_0 (\alpha^2 - \alpha^{-1}) \quad (6)$$

The D_0 factor which incorporates the structural features of the network chains, only reflects the "orientability" of the chain segments⁷⁾. Its values, which are of the order of $1/n$ (n being the number of bonds in the chain between two junctions), can be evaluated from the rotational isomeric state formalism by using a Monte Carlo chain generation technique. In eq.6, α is the extension ratio (ratio of the final length of the sample in the direction of stretch to the initial length before deformation) and \mathcal{P} is a factor equal to one for an affine network and $(1-2/\phi)$ for a phantom network, ϕ being the junction functionality.

The orientational behavior can be described by birefringence and by infrared dichroism. Birefringence is directly related to the second Legendre polynomial by the following expression :

$$\Delta n = [\Delta n]_0 \langle P_2(\cos\theta) \rangle \quad (7)$$

Both techniques are able to probe the orientational behavior of polymer chains at a molecular level, in contrast to the macroscopic information provided by most other characterization techniques.

According to the theory, the birefringence is related to the strain function by the expression^{8,9}:

$$\Delta n = \frac{\nu k T C}{V} \mathcal{P}(\alpha^2 - \alpha^{-1}) = D_1 (\alpha^2 - \alpha^{-1}) \quad (8)$$

where ν/V represents the number of chains per unit volume and C is the stress-optical coefficient which is related to the optical anisotropy Γ_2 of the network through the following equation :

$$C = \frac{2\pi (n^2+2)^2 \Gamma_2}{27 n k T} \quad (9)$$

n being the mean refractive index. C is usually referred to in the literature as the stress-optical coefficient since :

$$C = \Delta n / \sigma \quad (10)$$

where σ is the true stress (force f divided by the deformed area A) given by^{4,5} :

$$\sigma = \frac{\nu k T}{V} \mathcal{P}(\alpha^2 - \alpha^{-1}) \quad (11)$$

The absorption of infrared radiation is caused by the interaction of the electric field vector of the incident light with the electric dipole-transition moment associated with a particular molecular vibration⁷).

The parameter commonly used to characterize the degree of optical anisotropy in stretched polymers is the dichroic ratio R , defined as $R = A_{//} / A_{\perp}$ ($A_{//}$ and A_{\perp} being the absorbances

of the investigated band, measured with radiation polarized parallel and perpendicular to the stretching direction, respectively¹⁰⁻¹².

The orientation function is related to the dichroic ratio R by this expression :

$$\langle P_2(\cos \theta) \rangle = \frac{2}{(3\cos^2 \beta - 1)} \times \frac{(R-1)}{(R+2)} \quad (12)$$

where β is the angle between the transition moment vector of the vibrational mode considered and the local chain axis of the polymer.

Infrared measurements can be performed either in the mid- or in the near-infrared range¹³.

One practical problem in the case of infrared dichroism measurements arises from the requirement of band absorbance which should be roughly lower than 0.7 in order to permit use of the Beer-Lambert law although absorbances appreciably higher can be used with great care. That implies use of sufficiently thin films. Depending on the extinction coefficient of the considered band, the required thickness can range from 1 to 200 μm . From this point of view, polymers with strong absorption bands are difficult to study. This difficulty can now be overcome by using near-infrared (NIR) spectroscopy which examines overtones and combination bands much weaker than the fundamental modes.

The NIR region of the spectrum covers the interval from about 12500-4000 cm^{-1} (800-2500 nm). The bands in the NIR are primarily overtones and combinations of the fundamental absorbances found in the classical mid-IR region. The absorption bands appearing in the NIR range arise from overtones and combinations of fundamental vibrations of hydrogen-containing groups such as C-H, N-H and O-H. As these bands are much weaker than the corresponding fundamental absorptions, a NIR spectrum is considerably simplified compared to the usual mid-IR region. Consequently, the principal advantage of NIR analysis is the ability to examine specimens several mm thick. In other words, the NIR region which complements the mid-IR region, is analytically useful for spectroscopic applications involving analysis of samples containing very strong mid-IR absorbers¹⁴.

The data, reported in Fig.6, are related styrene-butadiene copolymers filled with silanized silica. They show that, at a given extension ratio, the second moment of the orientation function (derived from the dichroic ratios) or the birefringence of the matrix, increases with the filler content. This reveals a decrease in the apparent molecular weight between cross-links. It

is worth pointing out that similar behaviors are observed for silica-filled poly(dimethylsiloxane) networks¹⁵⁾.

The swelling and orientational measurements can be correlated since both techniques are sensitive to the total network density.

It has to be mentioned that, at high degrees of swelling, a series expansion of equation (3) leads to the following expression :

$$\frac{1}{M_c} \propto v_2^{5/3} = Q_{\text{rubber}}^{-5/3} \quad (13)$$

On the other hand, in infrared dichroism, the configurational factor has been shown to be proportional to $1/M_c$. Fig.7 shows that a good correlation is obtained between the two sets of data, the orientation being obtained whether by infrared dichroism or birefringence.

Fig.6 displays linear dependences of $\langle P_2(\cos\theta) \rangle$ or birefringence against the strain function. Plotting for a filled sample, orientation against stress, leads to a non-linear relationship, the increase in stress being larger at high deformations (Fig.8).

Limited chain extensibility

In the theory of rubber elasticity, the true stress σ (force divided by the deformed area) is given by equation 11^{4,5)}.

The quantity most often used to analyze results of stress-strain measurements in uniaxial deformation is the reduced stress $[\sigma^*] = \sigma / (\alpha^2 - \alpha^{-1})$ ^{17,18)} as suggested by the Mooney-Rivlin equation :

$$[\sigma^*] = 2C_1 + 2C_2 \alpha^{-1} \quad (14)$$

in which $2C_1$ and $2C_2$ are constants independent of α . $2C_1$ has been identified as the high-deformation modulus (the phantom network model limit) while $(2C_1 + 2C_2)$ is an estimate of the small strain modulus (the affine network model limit). So the phantom behavior is approached at large extensions ($\alpha^{-1} \rightarrow 0$).

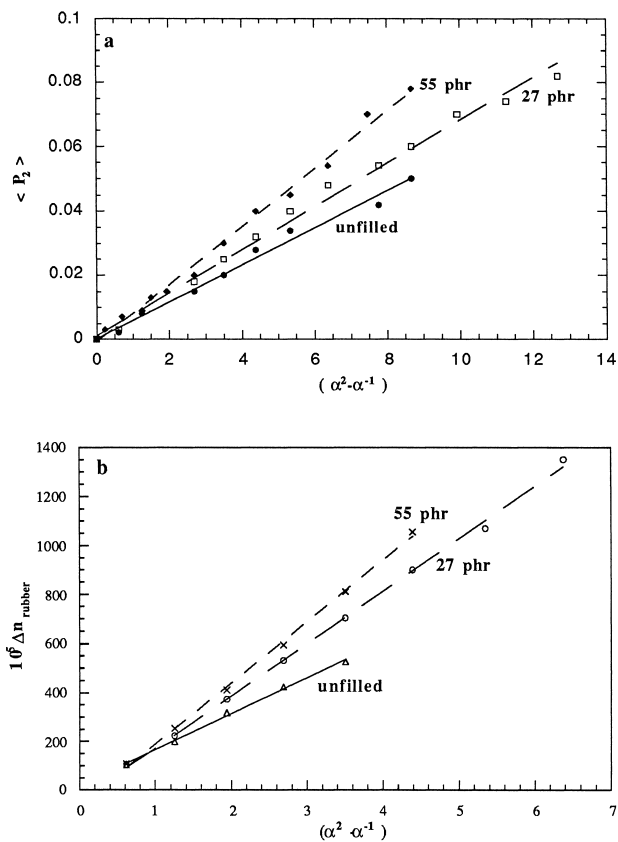


Fig.6: Chain orientation of polymer chains in styrene- butadiene copolymers filled with silanized silica : a : infrared dichroism; b : birefringence.

Typical Mooney-Rivlin for unfilled and filled networks are represented in Fig.9. While the unfilled network displays, at large deformations, a decrease in the reduced stress ascribed to the affine-phantom transition, the filled sample displays two additional effects :

- at low deformations, a decrease in the modulus attributed to the Payne effect,
- at high deformations, an upturn in the modulus due to limited chain extensibility.

It has to be mentioned that the polymer chains of the unfilled material also reach their limited chain extensibility but at a higher deformation.

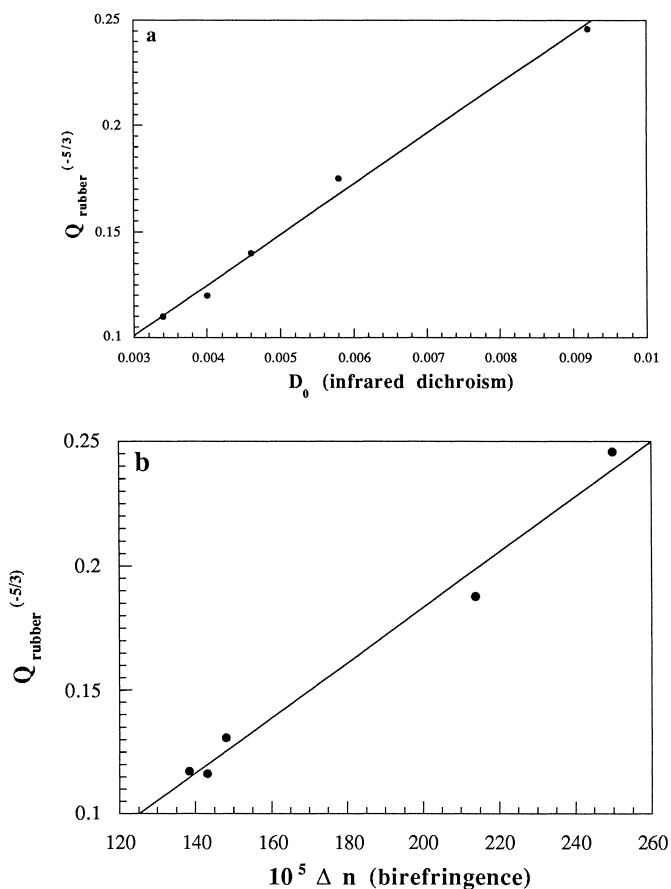


Fig.7: Correlation between swelling and orientational measurements for silica-filled styrene-butadiene copolymers.

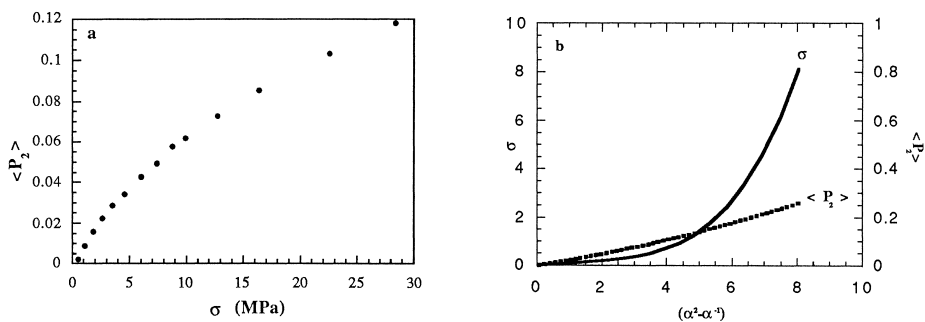


Fig.8: Relation between orientation and stress

a : experimental results; b : Monte Carlo simulation for chains containing 100 bonds between two junctions (from reference 16).

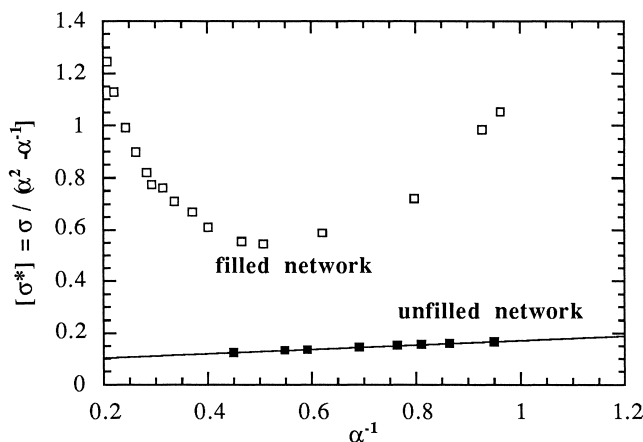


Fig.9: Mooney-Rivlin plots.

The upturn in the modulus, observed at high elongations in filled networks, is attributed to non-Gaussian effects caused by the finite (limited) extensibility of the short chains. This behavior is somewhat the signature of reinforcement and has something to do with unfilled bimodal networks consisting of short and relatively long chains linked together to the cross-linking agent. Such networks which are unusually tough, exhibit values of the modulus which increases very substantially at high elongations thus giving unusually large values of the ultimate strength¹⁹. The upturns in the modulus are due to the very limited extensibility of the short chains.

Strain amplification concept

The large increase in the modulus observed at large strains is due to non-Gaussian effects arising from limited extensibility of the short chains. Short chains, which provide a stiffening or reinforcement mechanism to the network, are essentially present in filler-rich and more aggregated areas of the sample.

Short chains reach values of the maximum extensibility by strain amplification effects caused by the inclusion of undeformable filler particles. In a two phase system of hard undeformable particles dispersed in a rubbery matrix, one can expect an effectively increased strain within the soft matrix (Fig.10). The so-called "strain amplification" factor relates the macroscopic

imposed strain state to the average strain state in the elastomer matrix material. Mullins and Tobin²⁰⁾ interpret the Guth and Gold function as a strain-amplification factor :

$$\epsilon_{\text{rubber}} = \epsilon_0 (1 + a\phi + b\phi^2), \quad (15)$$

where ϵ_{rubber} is the main local strain in the matrix and ϵ_0 the macroscopic strain. The Guth and Gold expression is an effective modulus expression and not a strain amplification relation.

An other expression, based on simple geometrical considerations, is given by Bueche²¹⁾ :

$$\alpha_{\text{rubber}} = \frac{\alpha - \phi^{1/3}}{1 - \phi^{1/3}} \quad (16)$$

where α_{rubber} is the extension ratio in the rubber material and α , the macroscopic extension ratio of the composite material.

The proper strain amplification is in fact :

$$\alpha_{\text{rubber}} = \frac{\alpha - \phi}{1 - \phi} \quad (17)$$

We have to note that the Bueche's expression is exact if we interpret the term $\phi^{1/3}$ as the line fraction of rigid segments in one-dimensional composite rod. On the other hand, this molecular reinforcement factor is generally understood in terms of an homogeneous overstrain in the matrix. Very recently, inhomogeneous strain field were demonstrated in silica-filled PDMS and SBR networks by atomic force microscopy. It was shown that an overstrain in the elastomerix matrix is obvious in filler-rich and more aggregated areas of the sample^{22,23)}. So the strain-amplification picture occurs occurs very locally.

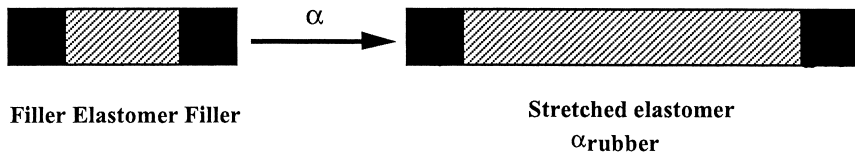


Fig.10: Schematic view of the strain amplification concept.

Infrared spectroscopy, by looking at specific absorption bands of the polymer chains, reveals that the average dimensions of the matrix itself, precisely the thickness e , obeys, under strain to a law of the type :

$$e_{\text{rubber}} = e_{0 \text{ rubber}} / \alpha^{1/2} \quad (18)$$

where $e_{0 \text{ rubber}}$ is the thickness of the elastomeric phase in the undeformed state. As it can be seen in Fig.11, the strain dependence of the thickness does not seem to be affected by overstrain effects.

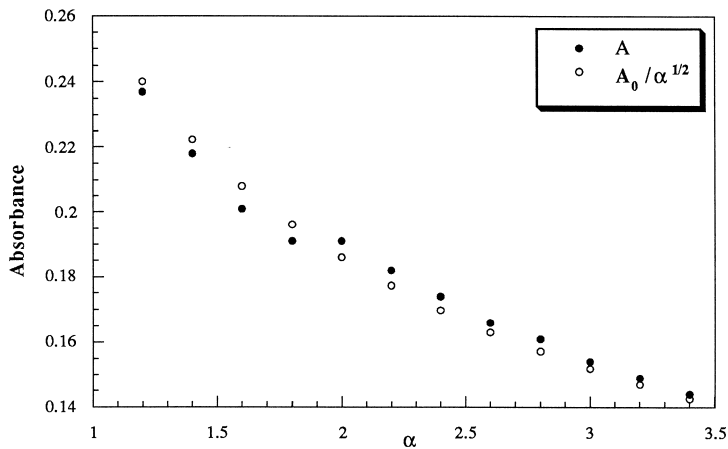


Fig.11: Strain dependence of the thickness of the elastomeric phase of a silica-filled styrene-butadiene copolymer.

Low strain dynamic behavior (Payne effect)

Another specific feature which cannot be overlooked in any discussion on filled elastomers, concerns the "Payne effect" characterized by this initial decrease in the modulus at small strains (Fig.12).

This effect is generally demonstrated through the strain dependance of dynamic mechanical properties of filled vulcanizates. Reinforced elastomers and more generally systems containing filler dispersions, are characterized by a non-linear viscoelastic behavior, known as the "Payne effect"^{24,25}. The strong decrease of the storage modulus G' , associated with a maximum of the loss modulus G'' , reveals an energy dissipation (Fig.12).

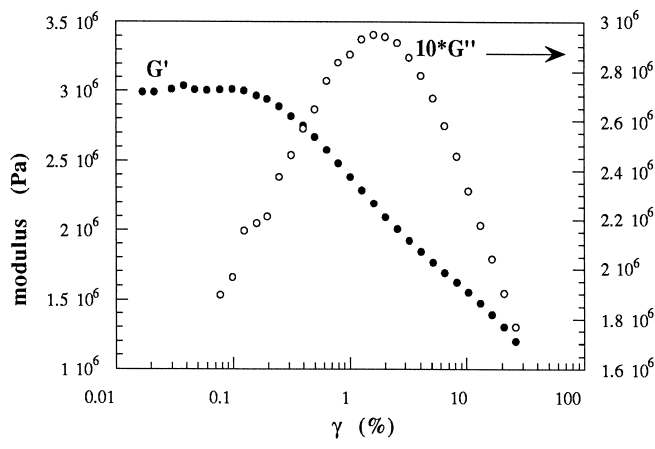


Fig.12: Description of the Payne effect.

The modulus drop ($\Delta G = G'_0 - G'_\infty$) with strain amplitude represents the Payne effect. At larger deformations, the difference between unfilled and filled rubber (G'_∞) contains the contribution arising from the inclusion of rigid particles (accounted for by the Guth and Gold expression) and also the contribution of the polymer-filler cross-links to the network structure²⁶) (Fig.13).

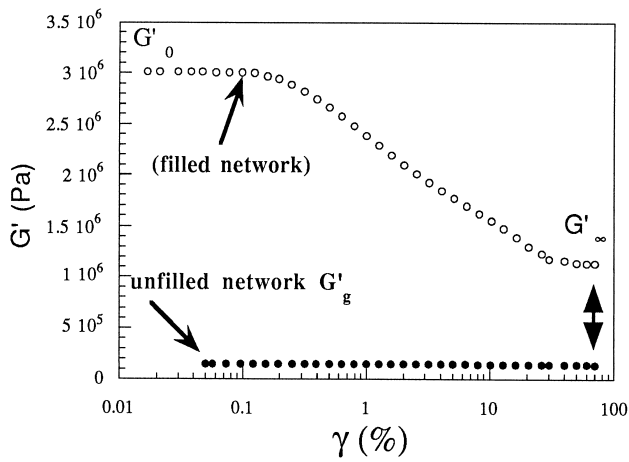


Fig.13: Strain dependence of G' for unfilled and filled rubbers.

The Payne effect increases with increasing filler loading. On the other hand, the dynamic properties of compounds as well as their temperature dependence are influenced by filler parameters like surface area, distribution and surface characteristics.

At a same filler loading and similar surface area, the Payne effect is much more important with silica than with carbon black (N110). The chemical modification of silica with Si69 reduces considerably the dynamic modulus²⁷⁾ (Fig.14).

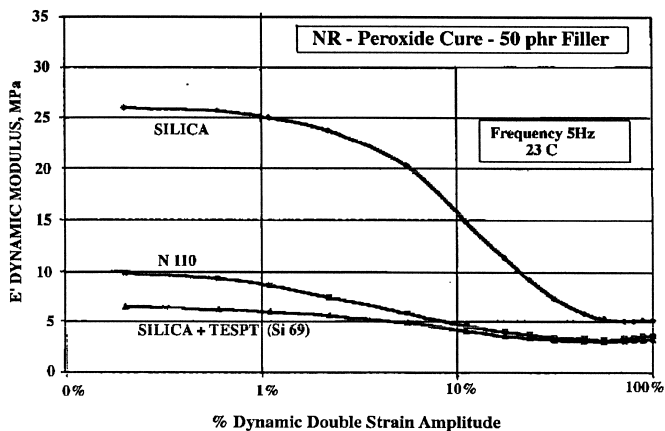


Fig.14: Strain dependence of E' for natural rubber (NR) filled with carbon black (N110), silica and TESPT-modified silica (From reference 27).

One parameter which plays an important role in the dissipation phenomena is the temperature. Fig.15 displays, for two different systems, a strong decrease of the storage modulus with increasing temperature. Of course, an opposite effect is expected from the theory of rubber elasticity which predicts that the modulus should increase with increasing temperature.

Payne²⁴⁾ believed that the strain dependencies of the moduli are essentially determined by the breakdown and reformation of the filler network. Under this assumption, the strain dependencies of both the viscous and elastic moduli have been modeled by Kraus²⁸⁾. Recently, Maier and Göritz²⁹⁾ have proposed a model of variable network density. This model, which is based on an adsorption mechanism, attributes the Payne effect to a desorption of the polymer chains from the particle surface.

Any of the two theoretical models is able to provide a perfect description of both moduli as a function of strain. Failure of each model may arise for incomplete assumptions, each of them

needing an additional mechanism. The Payne effect is probably determined by the filler network in combination with a mechanism originating at the polymer-filler interface. Further studies are in progress in order to elucidate the molecular mechanisms involved in the Payne effect.

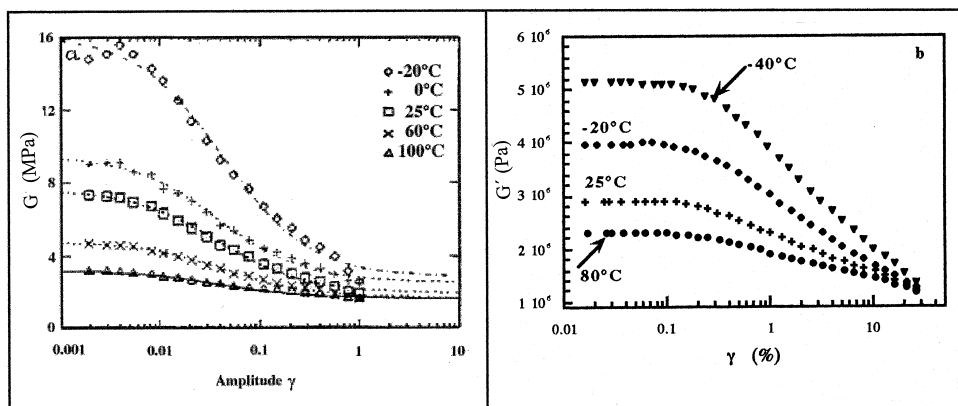


Fig. 15: Temperature dependence of the storage modulus:
a : SBR filled with 18.9% carbon black N339 (from references 29 and 30)
b : PDMS filled with 40 parts of silica (from reference 31).

Conclusion

Some specific features of filled elastomers are discussed. The author would like to emphasize that, a better insight into the reinforcement mechanisms of elastomers, can be obtained by combining several experimental techniques. Atomic force microscopy used for the characterization of filler microdispersion under strain promises to play an important role in the study of composite materials at a nanometer scale. On the other hand, spectroscopic techniques used to analyze the orientational behavior of filled systems or to characterize the filler surface, are able to provide a new area for understanding the molecular origin of the reinforcement effect.

References

1. E. Guth and O. Gold, *Phys. Rev.*, **53**, 322 (1938)
2. E. Guth, *J. Appl. Phys.*, **16**, 20 (1945)
3. P.J. Flory and J. Rehner, *J. Chem. Phys.*, **12**, 412 (1944)
4. J. E. Mark and B. Erman, *Rubber Elasticity. A molecular Primer*, Wiley-Interscience, New York (1988)
5. B. Erman and J. E. Mark, *Structure and Properties of Rubberlike Networks*, Oxford University Press, New York (1997)
6. B. Jasse and J.L. Koenig, *J. Macromol. Sci., Rev. Macromol. Chem.* **C17**, 61 (1979)

7. S. Besbes, I. Cermelli, L. Bokobza, L. Monnerie, I. Bahar, B. Erman and J. Herz, *Macromolecules*, **25**, 1949 (1992)
8. B. Erman, and P.J. Flory, *Macromolecules*, **16**,1601(1983)
9. B. Erman, and , P.J. Flory, *Macromolecules*, **16**,1607(1983)
10. B. Amram, L. Bokobza, J.P. Queslel, and L. Monnerie, *Polymer*, **27**,877 (1986)
11. B. Amram, L. Bokobza, L. Monnerie, J.P. Queslel, *Polymer*, **29**,1155 (1988)
12. L. Bokobza, B. Amram and L. Monnerie, *Elastomeric Polymer Networks*, (Eds J.E. Mark and B. Erman) Prentice Hall, New Jersey, 289 (1992)
13. T. Buffeteau, B. Desbat and L. Bokobza, *Polymer Communications*, **36**, 4339 (1995)
14. L. Bokobza, *J. Near Infrared Spectroscopy*, **6**,3 (1998)
15. L. Bokobza, F. Clément, L. Monnerie and P. Lapersonne, *The Wiley Polymer Networks Group Series*, (EdsK. te Nijenhuis and W.J. Mijs) John Wiley and Sons Ltd, 321 (1998)
16. L. Bokobza and B. Erman, *Macromolecules*, in press.
17. J. P. Queslel and J.E. Mark, *Encyclopedia of Physical Science and Technology*, **14**, 717 (1992)
18. J. E. Mark, *Polymer Journal*, **17**, 265, (1985)
19. J. G. Curro and J.E. Mark, *J. Chem. Phys.* **80**,9 (1984)
20. L. Mullins and N.R. Tobin, *J. Appl. Polym. Sci.*, **9**, 2993 (1965).
21. F.Bueche, *J. Appl. Polym. Sci.*, **4**, 107 (1960)
22. F. Clément, *Thèse de Doctorat*, Université Paris VI (1999)
23. A. Lapra, *Thèse de Doctorat*, Université Paris VI (1999)
24. A.R. Payne, *J. Polym. Sci.*, **6**, 57 (1962)
25. A. R. Payne and R. E. Whittaker, *Rubber Chem. Technol.*, **44**, 440 (1971)
26. A. R. Payne in : *Reinforcement of elastomers*, chap. 3. G. Kraus, ed. Interscience Publishers, New York (1965)
27. S. Wolff, *Rubber Chem. Technol.*, **69**, 325 (1996)
28. G. Kraus, *J. Appl. Polym. Sci., Appl. Polym. Symp.*, **39**, 75, (1984)
29. P.G. Maier and D. Göritz, *Kautschuk Gummi Kunststoffe*, **45**, 838 (1992)
30. A. C. Patel and D. C.Jackson, *Kautschuk Gummi Kunststoffe*, **49**, 18 (1996)
31. F. Clément, L. Bokobza, L. Monnerie and J. Varlet
Les Cahiers de Rhéologie, **XVI**,203(1998) and **XVI**,39 (1999)